Journal of Hazardous Materials, 23 (1990) 275–292
Elsevier Science Publishers B.V., Amsterdam — Printed in The Netherlands

THEORETICAL ANALYSIS AND EXPERIMENTAL EVALUATIONS OF THE BEHAVIOUR OF GRANULAR MOIST PIG IRON STOCKED IN THE PRESENCE OF AIR AND RELATED HAZARDS

GIUSEPPE GIORLEO

Dipartimento di Progettazione e Produzione Industriale, Facoltà di Ingegneria, Università di Bari, Viale Japigia 182, I 70126 Bari (Italy)

and

FRANCESCO GIOIA

Dipartimento di Ingegneria Chimica, Facoltà di Ingegneria, Università di Napoli, Piazzala Tecchio, I 80125 Naples (Italy)

(Received February 23, 1989; accepted in revised form February 5, 1990)

Summary

The influence of the chemical, physical and geometrical properties of a stockpile of moist granular pig iron on its self-heating, due to the reaction with air, is studied both theoretically and experimentally. Some of the hazards connected with the phenomenon are also examined.

The mathematical model describing the mass and heat transfer inside the pile has been solved and given are, among other things, the temperature and oxygen concentration profiles inside the pile. The analysis leads also to the definition of a critical size of the stockpile; for sizes smaller than this critical size the model developed confers a tool to control the behaviour of the system.

Specifically designed laboratory experiments have been conducted in order to evaluate some chemical, physical and geometrical parameters of interest. Moreover, the oxygen consumption is estimated and the hydrogen production is experimentally evidenced in a real case, for examining the related hazards.

1. Introduction

It is known that, when materials react exothermally with the oxygen contained in the air, safety problems may arise due to self-heating when these materials are either stored or transported in bulk.

Most attention has been devoted [1–3] to the case in which the self-heating of piles may degenerate, due to instability of the system, into self-ignition or even explosion. However, even when these limiting phenomena do not occur in the pile, safety problems may arise. The hazards may be due both to the primary reaction that consumes oxygen from the environment and to second-

0304-3894/90/$03.50

ary reactions producing explosive and/or poisonous gases. These secondary reactions, which can have negligible rates at room temperature, may become fast enough at the more elevated temperatures, though moderate, prevailing in the pile and therefore represent a serious source of hazard during transportation and storage.

The study of the problems that simultaneously involve transport phenomena (mass, heat and momentum) and chemical kinetics in an unsteady state situation, like that connected with a gas–solid reaction taking place in a bulk of porous material, is by its nature highly complex. A complete solution to the problem which accounts for transient terms, for instabilities and for all possible values of parameters is very difficult to obtain analytically. However, even though available, such a solution could be awkward to use in practice. Therefore, it is more realistic to study the specific problem at hand and to obtain solutions as a valid tool for controlling peculiar characteristics of interest. Obviously, the most appropriate simplifications are suggested by the physics of the case under study.

This approach is followed here for studying the behaviour of a pile of moist granular pig iron as regards its self-heating during storage and transportation. In particular, first the relevant parameters for pig iron are determined by specifically designed experiments. Secondly, a mathematical model based on the conservation of mass and energy equations is set; the solution, as regards temperature and oxygen concentration profiles, for different pile sizes and for different heat exchange situations, is obtained. Finally, with reference to the hazards, the rate of oxygen consumption is calculated and the hydrogen production is experimentally evidenced.

Some results are reported graphically in Figs. 3–6 to give immediate indications on the behaviour of the system under study.

2. Physical description

The system studied in the present paper is a pile of granular moist pig iron exposed to air, when stored and transported.

We can safely assume that the transformations taking place in this system regard only the external surface of the pig iron pellets (i.e., the pellet porosity effects are neglected). These transformations are essentially electrochemical in their nature and may be described by the overall reaction

$$2Fe + O_2 + 2H_2O \rightarrow 2Fe(OH)_2 \qquad (a)$$

Reaction (a) is exothermic ($\Delta H_a < 0$).

The ferrous hydroxide that forms by reaction (a) may decompose, at a rate increasing with temperature, according to the well-known Schikorr [4] reaction

$$3Fe(OH)_2 \rightarrow Fe_3O_4 + H_2 + 2H_2O \qquad (b)$$

Reaction (b) is endothermic ($\Delta H_b > 0$).

According to literature, e.g. [5], for the system explored in this work other reactions can be neglected.

Due to the granular structure of pig iron, oxygen diffuses inside the pile: reaction (a) takes place, the heat produced is transferred outside essentially by conduction, and temperature and concentration profiles are established in the pile. Actually, convective fluxes due to the change in number of moles, e.g. [6], and to natural convection induced by the exothermal reaction (a) [7] may also take place inside the stockpile. The effects of these convective fluxes, however, are neglected in this work because diffusion and heat conduction play a predominant role in the system as will be described below.

The problem at hand is strictly transient in nature because the pig iron is transformed as reaction (a) proceeds. However, because the reaction time of (a) is much longer than the characteristic time of mass and heat transfer, the processes taking place in the pile can be safely considered to be in a condition of pseudosteady-state. Consequently concentration and temperature profiles may be assumed constant over time. The pseudosteady-state assumption is discussed by Froment and Bischoff [8].

As far as the thermal effects are concerned (e.g. the temperature profiles that are established in the pile) it is reasonable to take into account only reaction (a) on the one hand. In fact reaction (b) has both a lower enthalpy (see next section) and a rate lower than that of reaction (a) at low temperatures ($T < 100\,^{\circ}C$, say).

On the other hand, as far as the chemical transformations are concerned, reaction (b) may also play a role. In fact, due to the heat generated by reaction (a), the temperature increases and reaction (b) may proceed at a significant rate (see also Section 9).

The temperature profiles that are established in the pile obviously depend on the characteristics of the system (e.g., rate of heat production, particle size distribution, geometry of the pile, boundary conditions). However, it should be pointed out that as long as water in its liquid state is present in the system (moist pig iron at atmospheric pressure) temperatures higher than $100\,^{\circ}C$ are not possible at any point in the pile. In fact at $100\,^{\circ}C$ a convective flow of water vapor starts purging from the inside to the outside of the pile thus inhibiting any significant diffusion of oxygen and production of heat. Naturally, if any point in the pile was or became dry, reaction (a) would not occur.

In conclusion, the pig iron pile warms up, oxygen is depleted and hydrogen forms. However, how much these effects represent a hazard in its storage and transportation obviously is related, among other things, to the conditions of venting.

3. Parameters characterizing the system

To study the problem under discussion, simultaneous mass, energy and momentum transport and chemical kinetics in a pile of granular pig iron, it is necessary to know the numeric values of many parameters (see Section 6).

Some of these parameters are characteristic of the specific material under study and not available from literature, so they have to be evaluated experimentally by specifically designed experiments and according to standard procedures. These entail the determination of:

- the effective pile density and (interstitial) void fraction;
- the moisture content;
- the effective thermal conductivity;
- the particle size distribution;
- the kinetic constant of reaction (a).

Other parameters, can be readily estimated from the data reported in literature. They are:

- enthalpy of reaction (a) and (b);
- effective diffusivity.

4. Experimental procedure

When not specified, standard methods were adopted.

4.1. Effective density and void fraction

The effective pile density, ϵ, and void fraction, α, obtained from experiment were 3100 kg/m^3 and 0.61, respectively.

4.2. Moisture content

The moisture content m was determined experimentally and amounted to 2.6% (0.026 kg of water/kg dry solid).

4.3. Effective thermal conductivity

The "observed" thermal conductivity of the moist granular pig iron is here measured utilizing a transient temperature method analogous to that reported by Sehr [9]. A spherical flask (5.8 cm radius) is filled with the material at 25°C (room temperature). The flask is then quickly placed in an oven maintained at a preset temperature of 80°C (a suitable temperature for the case under study) and the transient temperature at the center is measured by a thermocouple and recorded vs. time. The oven is a "Heraeus 5000", with forced air circulation and with a maximum temperature fluctuation of 0.8°C. The results for two runs are shown in Fig. 1 as the dimensionless temperature at the center of the flask, $(T-T_0)/(T_1-T_0)$, vs. time, where T is the tempera-

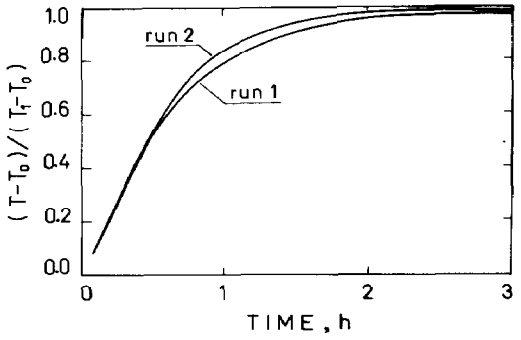

Fig. 1. Dimensionless temperature of pig iron at the center of the flask vs. time. T is the transient measured temperature, T_0 is the initial temperature (25°C) and T_1 is the temperature of the oven (80°C).

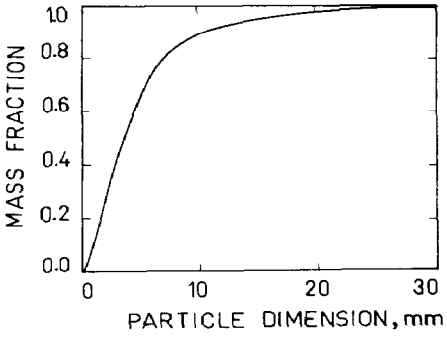

Fig. 2. Cumulative particle-size distribution plot for screen analysis of pig iron: mass fraction smaller than particle dimension reported in abscissa vs. particle dimension.

ture at the center of the flask, T_0 is the initial temperature of the material (25°C) and T_1 is the temperature of the oven (80°C).

These experimental curves have been worked out according to available theoretical equations of heat transfer, see e.g. [10,11]. The computational procedure, not reported here for brevity, yields an overall thermal conductivity coefficient, K_e, of 0.469 W/(m K). This is a typical value for granular material: note that for these materials the thermal conductivity does not depend strictly on the conductivity of the solid phase [12].

4.4. Particle-size distribution

The size analysis is made using the U.S. Standard Sieve Series (ASTM specification). The resulting cumulative particle-size distribution is reported in Fig. 2. Notice that from the size analysis it is possible to estimate the specific surface of each size fraction by the usual methods [13]. Adding up the size

fraction, the total specific area, a_w, for the pig iron under study is obtained $a_w = 0.403\ m^2/kg$.

4.5. Kinetic constant

Reaction (a) is a gas–solid reaction and its rate depends, among other things, on the reacting surface area. Therefore, assuming a first order kinetics in the oxygen concentration, the rate of reaction (a) expressed as moles of oxygen consumed per unit time and unit mass of pig iron, can be written as

$$r_a = -(dn/dt)/W = k_s a_w c \tag{1a}$$

This constitutive equation represents the overall mechanism of reaction (a). In fact it includes many reaction steps in series; i.e. adsorption, dissociation, chemical reaction, etc, but overall the reaction can be taken as first order.

The reaction rate based on the unit volume of granular pig iron pile is

$$\epsilon r_a = k_v c \tag{1b}$$

The first order kinetic constant k_s is related to the chemical nature of the reacting materials and the specific surface area a_w depends on the particle size distribution of the pig iron; k_v is a volume-based kinetic constant.

The relation between kinetic constant k (k_v or k_s) and temperature can be expressed by the Arrhenius equation

$$k = k^\circ \exp(-E/R_g T) \tag{2}$$

where R_g is the usual gas constant.

In order to evaluate the pre-exponential factor k° and the activation energy E in eqn. (2), the following specific experimental procedure is set up to measure k at several temperatures.

Assuming ideal gas behaviour and that the reaction takes place at constant volume and temperature, the reaction rate (in terms of oxygen gas pressure, p) may be written as

$$(dp/dt) = -(W/V) k_s a_w p \tag{3}$$

Equation (3) may be integrated with the boundary conditions

$$t = 0; \quad p = p_0 \tag{4}$$

$$t = t_1; \quad p = p_1 \tag{5}$$

to give

$$k_v = -\epsilon (V/W)(1/t_1) \ln(p_1/p_0) \tag{6}$$

and

$$p_1/p_0 = (79/21) \cdot y_1/(1 - y_1) \tag{7}$$

TABLE 1

Experimental parameters and resulting k_v's

Run#	W (kg)	$t_1 \cdot 10^{-4}$ (s)	T (K)	$y_1 \cdot 10^2$	$k_v \cdot 10^5$ (s^{-1})
1	1.000	7.20	311	13.3	4.43
2	1.300	6.66	333	6.3	9.03
3	0.920	8.64	354	6.0	10.48

The experimental procedure is as follows. A known amount (W, see Table 1) of the moist pig iron under study is loaded in a two-liter flask containing air. The flask is sealed, put in a Heraeus 5000 oven (already indicated) maintained at the preset reaction temperature reaction (a) starts. At the end of the run, the gas in the flask is sampled by a syringe and analyzed by an Oxygen Analyzer Taylor Servomex-OA.137. In this way the molar fraction of oxygen y_1 is measured (this value is confirmed by check calculations based on the measured final pressure in the flask) and k_v may be obtained by calculation.

The above procedure is followed for three different temperatures. The experimental parameters and the resulting calculated k_v are reported in Table 1. These data, regressed according to the Arrhenius law, yield.

$k_v^\circ = 0.064\ s^{-1}$ and $E = 1.86 \times 10^4$ J/mol

with a correlation coefficient of 0.952.

5. Estimated parameters

5.1. Enthalpy of reactions (a) and (b)

The enthalpy of reactions (a) and (b) at 25 °C, as calculated by the heats of formation reported in Perry's Chemical Engineers Handbook [14], are

$\Delta H_a = -565.5$ kJ/mol O_2 and $\Delta H_b = 17.4$ kJ/mol H_2

For the temperature changes encountered, the reaction enthalpies are assumed to be constant.

5.2. Effective diffusivity

For the pile of granular pig iron under study (neglecting the Knudsen diffusion) the effective diffusivity may be calculated as

$$D_e = \alpha D_{12}/q \tag{8}$$

where q is the tortuosity factor, for which the usual value, $\sqrt{2}$, is assumed. An acceptable average value of the free diffusion coefficient of oxygen in nitrogen is $D_{12} = 2.66 \times 10^{-5}$ m^2/s. Therefore by using eqn. (8) we obtain

$D_e = 1.15 \times 10^{-5}\ m^2/s$

5.3. Natural convection heat transfer coefficient

Natural convection represents a limiting case (characterized by a minimum value of h) which is usually encountered in pile storage. The usual size of pig iron piles (larger than one meter) is such that, for the purpose of estimating the natural convection coefficient, the effect of curvature may be neglected. Therefore a configuration is appropriate which corresponds to a horizontal heated plate facing upwards, in air at atmospheric pressure and at room temperature. According to the literature, e.g. [15], the relationship obtained is

$$h^* = 1.6(T_s - T_f)^{1/3} \tag{9}$$

6. Mathematical model

Spherical coordinates are used, as they seem the most appropriate to describe the geometry of usual piles. However, for geometries other than spherical, according to Aris [16] an equivalent radius can be defined as the ratio between the volume and the external surface of the pile. Therefore, the results obtained in this work can also be applied to different geometries satisfactorily.

With reference to oxygen, whose rate of disappearance is given by eqn. (1b), the conservation of mass and energy equations for a differential spherical shell of radius r and thickness dr are, respectively

$$(D_e/r^2)\,d(r^2 dc/dr)/dr - k_v c = 0 \tag{10}$$

$$(K_e/r^2)\,d(r^2 dT/dr)/dr - \Delta H_a k_v c = 0 \tag{11}$$

Boundary conditions are at $r = 0$,

$$dc/dr = dT/dr = 0 \tag{12}$$

because of symmetry, and at $r = R$,

$$k_c(c_s - c_f) = -D_e(dc/dr)_{r=R} \tag{13a}$$

$$h(T_s - T_f) = -K_e(dT/dr)_{r=R} \tag{13b}$$

for continuity.

In the mass balance, eqn. (10), both the convective flux due to the change in number of moles produced by reaction (a) and the effect of hydrogen production by reaction (b) are neglected.

In dimensionless form eqns. (10) and (11) become

$$d^2\Gamma/d\sigma^2 + (2/\sigma)d\Gamma/d\sigma - \Phi^2(\Gamma+1)\exp[\phi\Theta/(\Theta+1)] = 0 \tag{14}$$

$$d^2\Theta/d\sigma^2 + (2/\sigma)d\Theta/d\sigma - \beta\Phi^2(\Gamma+1)\exp[\phi\Theta/(\Theta+1)] = 0 \tag{15}$$

the boundary conditions being at $\sigma=0$,

$$d\Gamma/d\sigma=0 \tag{16a}$$

$$d\Theta/d\sigma=0 \tag{16b}$$

and at $\sigma=1$,

$$(Bi)_m\Gamma_s=-(d\Gamma/d\sigma)_{\sigma=1} \tag{17a}$$

$$(Bi)_h\Theta_s=-(d\Theta/d\sigma)_{\sigma=1} \tag{17b}$$

where Γ is the concentration, Θ the temperature, σ the radial coordinate, β the Prater temperature, ϕ the Arrhenius number, Φ the Thiele modulus, and Bi the Biot number, all in dimensionless form. Subscripts $_h$ and $_m$ denote respectively heat and mass. The dimensionless parameters are defined in eqn. (18).

$$\Gamma=(c-c_f)/c_f; \qquad \Theta=(T-T_f)/T_f; \quad \sigma=r/R$$

$$\beta=\Delta H_a c_f D_e/K_e T_f; \quad \phi=E/R_g T_f; \qquad \Phi=\sqrt{R^2 k_{vf}/D_e} \tag{18}$$

$$(Bi)_m=k_c R/D_e; \qquad (Bi)_h=hR/K_e$$

Combining eqns. (14) and (15), integrating and using eqns. (17) gives

$$\Gamma=(1/\beta)\,[\Theta-\Theta_s(1-1/\Pi)] \tag{19}$$

where

$$\Pi=(Bi)_m/(Bi)_h \tag{20}$$

In order to obtain the temperature profiles in the pile, eqn. (19) is substituted into eqn. (15) and gives

$$d^2\Theta/d\sigma^2+(2/\sigma)d\Theta/d\sigma=\Phi^2[\beta+\Theta-\Theta_s(1-1/\Pi)]\exp[\phi\Theta/(\Theta+1)] \tag{21}$$

Typical values of Π are ≈ 100 [17], so that eqn. (21) may be simplified to give

$$d^2\Theta/d\sigma^2+(2/\sigma)d\Theta/d\sigma=\Phi^2(\beta+\Theta-\Theta_s)\exp[\phi\Theta/(\Theta+1)] \tag{22}$$

Equation (22) with the Boundary conditions (16b) and (17b) leads to a mathematical description of the system under study.

For exothermal reactions, where the heat produced must be balanced by the heat removed, problems of multiple solutions may arise and the steady-state behaviour may not be sufficiently defined by the present approach. A thorough and comprehensive analysis, including study of the stability conditions, is reported by Aris [17]: in particular it is shown that the condition for uniqueness of the steady-state solution is controlled by the actual values of the β and ϕ parameters. The values of β and ϕ reported in the next section assure the stability of the system.

The approach previously described is encountered in the literature for the study of reactions in porous catalysts and the results are usually reported in

terms of effectiveness factor vs. Thiele modulus. In this paper, on the other hand, the numerical integration of eqn. (22) yields the temperature profiles (and eqn. (19) those of concentration) in the pile and the rate of oxygen consumption. In this way an expedient tool is obtained to control, among other things, safety conditions in transportation and storage of moist granular pig iron in bulk.

In particular the molar rate of oxygen consumption in the pile is

$$Q = 4\pi R^2 D_e (dc/dr)_{r=R} \tag{23}$$

and, making use of eqns. (18) and (19), the volumetric rate of oxygen consumption at standard conditions may be calculated by

$$Q_v = -0.25R(d\Theta/d\sigma)_{\sigma=1} \quad Q_v[=]\,m^3/h,\ R[=]\,m \tag{24}$$

7. Values of the dimensionless groups

Using the values of the parameters which have been previously obtained, one gets the following values of the relevant dimensionless group defined by eqn. (18)

$$\beta = -0.40, \quad \phi = 7.51, \quad \Phi^2 = 3.06R^2;\ R[=]\,m \tag{25}$$

where it is assumed $T_f = 298$ K and $c_f = 8.89 \times 10^{-3}$ kmol/m^3 (standard air).

For the Biot number a range of practical usage for the case considered here must be defined.

The lower limit of the thermal Biot number is the one pertaining to natural convection, $(Bi)_{h^*}$, and it is calculated, by using eqn. (9) by

$$(Bi)_{h^*} = 22.79\Theta_s^{1/3} R;\ R[=]\,m \tag{26}$$

With regard to the upper limit of $(Bi)_h$, it is obvious that, since as $(Bi)_h \to \infty$, $T_s \to T_f$, there must exist a suitable value for the Biot number, above which $T_s = T_f$ is a reasonable approximation and the external resistances may be neglected. In particular, the parameter

$$\delta = (T_{max} - T_s)/(T_{max} - T_f) = (\Theta_{max} - \Theta_s)/\Theta_{max} \tag{27}$$

which is the temperature drop in the pile as a fraction of the total temperature difference, gives a quantitative indication of the relative importance of external heat transfer resistances. Therefore, an acceptable upper limit for $(Bi)_h$ can be based on a suitable value for δ. Assuming that the external resistances may be considered negligible when $\delta \geq 0.98$, the numerical results reported below show that $(Bi)_h = 100$ is an acceptable upper limit for the Biot number, for the case under study.

For the range of temperatures occurring in this work, it is reasonable to assume that all the above dimensionless groups are constant with temperature.

8. Results of integration and discussion

The results of the numerical integration of eqn. (22) are reported in Figs. 3–6. For the present case, as previously underlined in Section 2, the results obtained have physical validity only below $T=100\,^{\circ}C$ ($\Theta=0.25$).

Figure 3 refers to heat transfer by natural convection only. Natural convection requires particular attention because, besides being a limiting case, it represents the most hazardous condition, as it is characterized by the highest temperatures within the pile. The range of pile radii reported is 0.5–5 meters. The following comments on the curves of Fig. 3 are obviously based on the assumption that h^* (see eqn. 9) does not depend on the pile radius, R, in practice.

In Fig. 3(a) Θ_s, Θ_{max} and δ are reported vs. R. With reference to Θ_s and Θ_{max} one should note that the heat exchanged with the surroundings always depends on the external surface of the pile (which is of course proportional to R^2). On the other hand: i) at the lower values of the radius, the reaction and the heat produced involve the whole volume of the pile (proportional to R^3) and consequently Θ_s and Θ_{max} increase, with Θ_{max} increasing faster, as R grows; ii) for the greater values of R, the reaction and the heat produced involve only a peripheral thin shell of the pile of constant thickness, $\sqrt{D_e/k_{vf}}$: therefore both the heat produced and that exchanged are proportional to the external surface

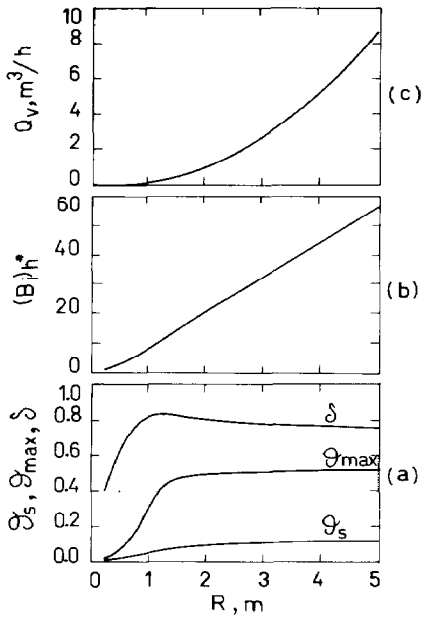

Fig. 3. Dimensionless quantities (a), Biot number for natural convection (b) and standard volumetric rate of oxygen consumption in the pile (c) vs. radius.

and thus Θ_s and Θ_{max} will remain practically constant. With reference to δ, the relative curve has a behaviour similar to that at the above two temperatures, Θ_s and Θ_{max}, but a maximum is present in the transition zone. This maximum is due to the same thermal effects which produce maxima in the curves of effectiveness factors vs. Thiele modulus [17]. Finally, inspection of the Θ_{max} curve shows that the physical limit $\Theta=0.25$ implies a corresponding critical size value.

Figure 3(b) reports the Biot number for natural heat convection, $(Bi)_{h^*}$, as a function of the radius of the pile. The behaviour is approximately linear because h^* can be assumed not to depend on R.

Figure 3(c) reports the volumetric rate of oxygen consumption, Q_v, vs. R. Notice that when the reaction is confined to the peripheral thin shell of the pile, Q_v depends on the external surface and its behaviour is that observed in the Figure.

Figure 4 gives a few temperature profiles inside the pile for values of the parameters $(Bi)_h$ and R of particular interest. For each R value, the family of profiles parametric in the Biot number, from $(Bi)_{h^*}$ to $(Bi)_h=100$, are reported. It is interesting to notice that, consistently with the choice made for the upper limit of the Biot number, the higher Biot number curves tend to collapse onto each other. Furthermore, as discussed under Fig. 3(a), as R becomes greater the profiles show a flat zone in the core of the pile indicating that the reaction does not involve all of the volume.

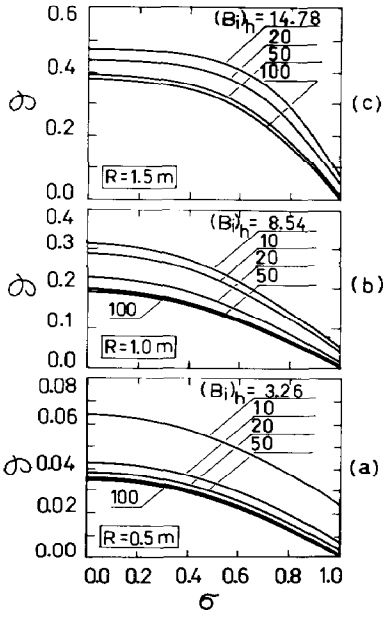

Fig. 4. Dimensionless temperature vs. dimensionless radial coordinate; for $R=0.5$ m (a), $R=1.0$ m (b) and $R=1.5$ m (c).

Figures 4(a), 4(b) and 4(c) report the three possible cases with reference to R.

Figure 4(a) reports the case ($R=0.5$ m) for which Θ never exceeds 0.25, for all possible situations of heat exchange with the surroundings. Therefore the model permits a complete control of the system.

Figure 4(b) represents a case ($R=1$ m) for which a few curves cross $\Theta=0.25$. Naturally only the curves lying completely under 0.25 have physical meaning and can be used in the case under study.

Figure 4(c) reports a case ($R=1.5$ m) for which all curves cross 0.25. In this case the curves, even though they represent in general the behaviour of a reacting system, cannot be used in the present case (different transport equations are necessary to model the phenomenon) and are reported for completeness.

Figure 5 reports Θ_s, Θ_{max} and δ vs. $(Bi)_h$ for different R values. All curves have different starting points and the loci of these points correspond to the curves of Figure 3(a). Because the efficiency of the heat transfer increases, Θ_s and Θ_{max} decrease. Furthermore

$$(Bi)_h \to \infty, \quad \Theta_s \to 0 \tag{28}$$

and, as suggested by eqn. (19),

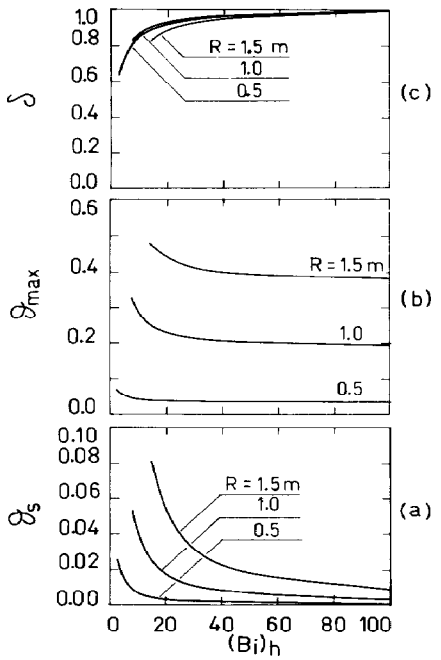

Fig. 5. Dimensionless quantities $\ll \Theta_s$ (a), Θ_{max} (b) and δ (c) $\gg$ vs. Biot number, for different values of R.

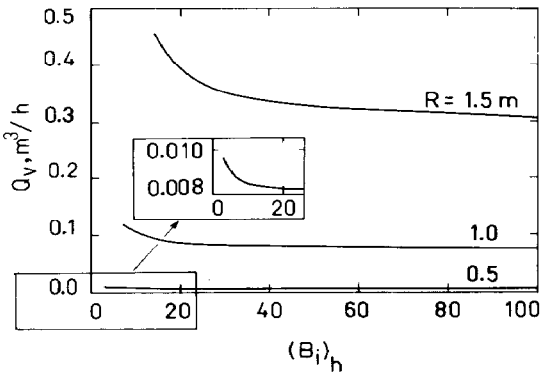

Fig. 6. Standard volumetric rate of oxygen consumption in the pile vs. Biot number, for different values of R.

$$(Bi)_h \to \infty, \quad \Theta_{max} \to \beta \Gamma_{min} \tag{29}$$

where $\Gamma_{min} = \Gamma(\sigma = 0)$. When $R \to \infty$, $\Gamma_{min} \to -1$ and therefore

$$(Bi)_h \to \infty \text{ and } R \to \infty, \quad \Theta_{max} \to -\beta \tag{30}$$

The behaviour of δ for any R can be deduced from the corresponding behaviour of Θ_{max} and Θ_s, considering also that for $(Bi)_h \to 0$, $\Theta_s \to \Theta_{max}$. In short, the family of δ curves are consistent with Figure 3(a). Finally, Fig. 5(b) gives an indication of the existing correlation between the critical size and the Biot number.

Figure 6 reports Q_v vs. $(Bi)_h$ for different R values. The oxygen consumption rate, Q_v, is a measure of the total reaction taking place inside the pile. Since the reaction rate is an exponential function of temperature, while it is a less strong function (linear in the case at hand) of concentration, the effect of any temperature change may overcome the effect of the consequent concentration change. Therefore the behaviour of Q_v will be similar to that of the temperatures reported in Fig. 5. Finally, all curves of Fig. 6 have different origins and the locus of these points corresponds to the curve of Figure 3(c).

9. Experimental evidence and safety considerations

Apart from the previous experimental measurements obtained in the laboratory in order to estimate the physical parameters of granular pig iron, an experimental investigation into the same material has been made also on an unconditioned stocked moist pile (approximately hemispheric) of about 6 meters radius confined in a place of 2250 m^3 total volume.

9.1. Temperature measurement

This pile was warm and water vapor emanating from the external surface was visible. The temperature measured at two different penetration depths in

TABLE 2

Explosion hazard assessment of an unconditioned moist granular pig iron stockpile by means of an explosimeter

t, h	% L.E.L.
0	30
5	35
25.5	60

the pile (30 cm and 60 cm) was found to be very close to 100°C in both cases. This experimental result is consistent with the analysis developed above. In fact, the mathematical model suggests the existence of a critical size of the pile for which the maximum temperature in the pile is 100°C. This size depends on the Biot number and for natural convection it is about one meter (see Fig. 2). Evidently, for larger radii, temperatures very close to 100°C are present inside the pile as long as liquid water is present.

9.2. Hydrogen production

Three measurements of explosivity in the air surrounding the pile were made, at different times, by an a "MSA explosimeter model 2E". As known this instrument gives the concentrations of flammable gases expressed as a percentage (by volume) of the lower explosive limit (% L.E.L.). The first measurement was made at an arbitrary zero time; the other two values were taken after 5 and 25.5 hours, respectively. The result is given in Table 2.

For hydrogen the L.E.L. is 4 vol.%, e.g. [18]. Therefore, the amount of hydrogen present in the ambient air may be estimated.

These figures indicate that a dangerous situation may build up and that reaction (b) cannot be neglected and for each individual case a model should be made for the evaluation and the control of the hazards in the storage and transportation of granular pig iron.

Conclusions

The approach followed in this paper suggests a method for studying the behaviour of granular material in bulk, when transport phenomena and chemical reactions take place simultaneously. The theoretical and experimental analyses, however, are in particular developed for the study of moist pig iron stockpiles and the related hazards. Since this system is characterized by the presence of liquid water, 100°C is a limit temperature and a corresponding critical size (radius) exists, which is about one meter in the case of natural convection. This value is in good agreement with the previously obtained experimental evidence. Below this physical limit the model applies and predicts the behav-

iour of the system (e.g., the temperature profile in the pile, the rate of oxygen consumption, the hydrogen produced and the consequent safety conditions).

When the water vapor pressure equals the prevailing pressure, a convective flux starts from the inside towards the outside of the pile. This new phenomenon could invalidate eqns. (10) and (11), which describe the oxygen transport as taking place exclusively by diffusion, and therefore a different model is required. The study of this different approach is in progress.

Notation

a_v	ϵa_w	m^2/m^3
a_w	specific surface per unit mass of particulate pig iron	m^2/kg
$(Bi)_h$	Biot number for heat transfer, hR/K_e	—
$(Bi)_{h^*}$	Biot number for natural convection heat transfer, h^*R/K_e	—
$(Bi)_m$	Biot number for mass transfer, k_cR/D_e	—
c	oxygen concentration	$kmol/m^3$
c_f, c_s	values of c in the core of the fluid and on the surface of the pile, respectively	$kmol/m^3$
D_{12}	diffusivity coefficient for free diffusion of oxygen in nitrogen	m^2/s
D_e	effective diffusivity	m^2/s
E	activation energy of reaction (a)	kJ/kmol
ΔH_a, ΔH_b	enthalpy of reactions (a) and (b) at 25 °C	kJ/mol
h	heat transfer coefficient	$W/(m^2K)$
h^*	natural convection heat transfer coefficient	$W/(m^2K)$
K_e	effective thermal conductivity of pig iron pile	W/(m K)
k	kinetic constant	see k_s, k_v
k°	pre-exponential factor dimensions as those of the corresponding k	dim(k)
k_c	mass transfer coefficient	m/s
k_s	surface-based kinetic constant	m/s
k_v	volume-based kinetic constant, $k_v = \epsilon k_s a_w$	s^{-1}
k_{vf}	k_v at $T = T_f$	s^{-1}
m	moisture content	—
n	number of oxygen moles	kmol
p	oxygen partial pressure	kPa
p_0, p_1	oxygen partial pressure at $t=0$ and $t=t_1$	kPa
q	tortuosity factor	—
Q	molar rate of oxygen consumption in the pile	kmol/s
Q_v	standard volumetric rate of oxygen consumption in the pile	m^3/h

R	radius of the pile	m
R_g	gas constant, 8.3144	kJ/(kmol K)
r	radial coordinate	m
r_a	rate of reaction of oxygen per unit mass of pig iron	(kmol/kg s)
T	temperature	K
T_0, T_1	temperatures, see Fig. 1	K
T_f, T_s	temperatures in the core of the fluid and on the surface of the pile, respectively	K
T_{max}	maximum temperature in the pile (at the center)	K
t	time	s
t_1	final time, reaction time see eqn. (6)	s
V	gas phase volume in the flask	m^3
W	mass of pig iron loaded into the flask	kg
y_1	oxygen molar fraction at $t=t_1$	—

Greek symbols

α	void fraction of the pile	—
β	Prater temperature, see eqn. (18)	—
Γ	dimensionless concentration, see eqn. (18)	—
δ	fraction of temp. drop in the pile, see eqn. (27)	—
ϵ	effective density of pig iron pile	kg/m^3
σ	dimensionless radial coordinate	—
Φ	Thiele modulus, see eqn. (18)	—
π	$(Bi)_m/(Bi)_h$	—
Θ	dimensionless temperature, see eqn. (18)	—
Θ_{max}	dimensionless temperature at $\sigma=0$	—
Θ_s	dimensionless temperature at $\sigma=1$	—
ϕ	Arrhenius number, see eqn. (18)	—

References

1 D.A. Frank-Kamenetskii, Diffusion and Heat Exchange in Chemical Kinetics (translated by J.P. Appleton), Plenum Press, New York, 2nd edn., 1969.
2 P.C. Bowes, Self-heating: Evaluating and Controlling the Hazards, HMSO, London, 1984.
3 K. Brooks, V. Balakotaiah and D. Luss, Effect of natural convection on spontaneous combustion of coal stockpiles, AIChE J., 34 (1988) 353-365.
4 G. Schikorr, Über die Reaktionen zwischen Eisen seiner Hydroxyden und Wasser, Zeitschr. Elektrochem., 35 (1929) 65-70.
5 J. Bénard, L'Oxydation des Métaux, Gauthier-Villars (Editeur), Paris, 1964.
6 A. Burghardt and J. Aerts, Pressure changes during diffusion with chemical reaction in a porous pellet, Chem. Eng. Process., 23 (1988) 77-87.

7 W. Kordylewski and Z. Krajewski, Convection effects on thermal ignition in porous media, Chem. Eng. Sci., 39 (1984) 610-612.
8 G.F. Froment and K.B. Bischoff, Chemical Reactor Analysis and Design, John Wiley, New York, 1979, pp. 242-243.
9 R.A. Sehr, The thermal conductivity of catalyst particles, Chem. Eng. Sci., 9 (1958) 145-152.
10 R.B. Bird, W.E. Stewart and E.N. Lightfoot, Transport Phenomena, John Wiley, New York, NY, 1960, pp. 352-364.
11 D.Q. Kern, Process Heat Transfer, McGraw-Hill/Kogakusha, Tokyo, 1950, p. 654.
12 R.A. Mischke and J.M. Smith, Thermal conductivity of alumina catalyst pellets, Ind. Eng. Chem. Fundam., 1 (1962) 288-292.
13 A.S. Foust, L.A. Wenzel, C.W. Clump, L. Maus and L.B. Andersen, Principles of Unit Operations, John Wiley, New York, NY, 1960, pp. 525-538.
14 R.H. Perry, D.W. Green and J.O. Maloney (Eds.), Perry's Chemical Engineers Handbook, 6th edn., McGraw-Hill, New York, NY, 1985, p. 3-147.
15 F. Kreith, Principi di trasmissione del calore, (Principles of heat transfer) Liguori (Ed.), Napoli, 1974, pp. 393-398, 630.
16 R. Aris, On shape factors for irregular particles-I. The steady state problem. Diffusion and reaction, Chem. Eng. Sci., 6 (1957) 262-272.
17 R. Aris, The Mathematical Theory of Diffusion and Reaction in Permeable Catalysts, Vols. I and II, Clarendon Press, Oxford, 1975.
18 R.C. Weast, CRC Handbook of Chemistry and Physics, CRC Press, Inc., Boca Raton, FL, 1987.